Noname manuscript No.
(will be inserted by the editor)

Signatures of attractive and repulsive interactions on quantum correlations in the Hubbard Model

Andrea Beggi · Luca Razzoli · Paolo Bordone

Date: 15-04-2016

arXiv:1605.07513v1 [quant-ph] 24 May 2016

Abstract We study the dynamics and the entanglement between two interacting identical bosons performing a quantum walk on a 1D lattice. The system is described by the Hubbard model, and the interaction among the particles can be either attractive or repulsive. We show that there are clear signatures – both in the evolution and in the correlations – that allow a distinction between the two cases, and we demonstrate that these features result to be intimately connected with the bandstructure and the eigenstates of the Hubbard Hamiltonian.

Keywords Indistinguishable particles · Entanglement of particles · Bose-Hubbard model · Attractive and repulsive interactions

PACS 03.65.Ud · 03.67.-a · 03.67.Mn · 71.10.Fd · 03.75.Lm

1 Introduction

Quantum walks (QWs) describe the random dynamics of a quantum particle on a lattice [1, 2]. They show characteristic quantum features with respect to their classical counterpart - such as ballistic propagation, coherent superposition and interference of the wavefunction. These effects make QWs extremely promising for the implementation of quantum algorithms that are faster and more efficient with respect to the protocols traditionally adopted in classical computation [3–5], since they rely on entanglement or other quantum correlations. The potential applications in the field of quantum information inspired a series of recent experimental investigations, which focused on systems such as optical networks and quantum optics [6–8], nuclear magnetic resonance, ionic or atomic traps, and quantum-dot arrays (for a recent review see [9]). In detail, some experimental realizations of photonic quantum walks (photonic chips) have been achieved lately [7, 10–12], and it was shown that they are capable to act as quantum computing architectures that outperform classical computers in some specific tasks.

In these systems, QWs are typically performed by identical particles, which show very peculiar features: indeed, it has been demonstrated that the indistinguishability of the walkers can build up genuinely quantum correlations even in the absence of interaction between the particles [13, 14], as it was observed experimentally in photonic waveguides [6, 7, 15]. The entanglement among identical particles has raised a lot of interest in recent times, since it is crucial for understanding many physical phenomena which involve highly correlated indistinguishable subsystems. However, despite large research activities [16–34], there isn't yet a well defined formulation for the quantification of this entanglement. Among the many criteria that have been proposed, the so-called *entanglement of particles* by Wiseman and Vaccaro [24] is one of the most promising, due to its simple computability, and to the fact that it should be physically measurable in many experimental scenarios [25]. Indeed, it has been recently employed for estimating quantum correlations in spin chains [35, 36] - where it is able to detect quantum phase transitions - and in model systems of QWs described by the Hubbard Hamiltonian [14, 37, 38].

A. Beggi, L. Razzoli, P. Bordone
Dipartimento di Scienze Fisiche, Informatiche e Matematiche, Università di Modena e Reggio Emilia
Via Campi 213/A, I-41125, Modena, Italy
P. Bordone
Centro S3, CNR-Istituto di Nanoscienze Modena
Via Campi 213/A, I-41125, Modena, Italy
E-mail: andrea.beggi@unimore.com

The Hubbard Hamiltonian [39–41], despite its simplicity, is one of the most general models for systems of correlated fermions or bosons [42] – e.g. Mott insulators, high-temperature superconductors, ultracold atomic lattices [43–46], spin chains [47, 48] and nonlinear waveguide lattices [49–53] – and in the limit of large interactions it can be mapped onto the XXZ Heisenberg model [47, 54]. More specifically, the Hubbard model can be used to describe QWs of (interacting) identical particles [55–58], where the interaction can be both attractive or repulsive, depending on the chosen physical implementation; for some systems, both possibilities are contemplated [50, 59–61].
Recent experimental results on cold atoms in an optical lattice showed that a bounded couple of interacting particles can be formed even under the action of a repulsive potential [43, 60, 62–64]. This phenomenon has a clear physical explanation by looking at the bandstructure of the model, which behaves symmetrically under the exchange of sign in the interaction term: for both attractive and repulsive potentials, the onset of the interaction creates a separate miniband hosting bounded states, thus determining the co-walking of the particles that are initially placed on the same site [49, 65]. This first interesting result suggested that the behaviour of the model is totally symmetrical under the exchange of sing of the interaction, and some following works [49] pointed out that there are no differences in the correlations among particles when the interaction potential switches from positive to negative values.
However, a recent study [38] on entanglement among identical bosons in a quantum walk showed that, for some specific initial states, the Hubbard model induces a different evolution for attractive and repulsive interactions. This dependence of correlations upon the interaction could be exploited in the next future, in order to engineer the enetanglement among the walkers at a deeper level, granting us a further degree of freedom for performing quantum computing tasks with quantum walks.
In this paper we characterize the dynamical evolution of the state and the entanglement of a pair of interacting bosons through numerical simulations. We show that the sign of the interaction affects both the walker dynamics and their correlations and we develop an explanation for this behaviour.
The paper is organized as follows: in Sect. 2 we introduce the bosonic Hubbard-model and the theoretical tools that we used to quantify the entanglement between the walkers. Section 3 reports the results of our numerical simulations on a chain with $N = 30$ sites, which are then discussed in Sect. 4 through the help of a simplified semi-analytical model (a reduced chain with $N = 4$ sites). Finally, Sect. 5 sums up the conclusions of our work and advances some further perspectives of research.

2 Theoretical Model

2.1 Bose-Hubbard model

The Bose-Hubbard Hamiltonian describes a collection of spinless bosons hopping between the N sites of a 1D chain, typically with periodic boundary conditions ($N + 1 = 1$). In the second quantization formalism (and for $\hbar = 1$), it is given by:

$$\hat{\mathcal{H}}_N(J,V) = -J\sum_{i=1}^{N}\left(\hat{c}_{i+1}^{\dagger}\hat{c}_i + \hat{c}_i^{\dagger}\hat{c}_{i+1}\right) + \frac{V}{2}\sum_{i=1}^{N}\hat{n}_i(\hat{n}_i - 1), \tag{2.1}$$

where J is the hopping amplitude, and V is the strenght of the interaction among the bosons sharing the same site (attractive for $V < 0$, repulsive for $V > 0$). In this paper, we are considering a system with total number of particles $n = 2$. The Hamiltonian can be rewritten as

$$\hat{\mathcal{H}}_N = J\,\hat{h}_N(v) = J\left(-\sum_{i=1}^{N}\left(\hat{c}_{i+1}^{\dagger}\hat{c}_i + \hat{c}_i^{\dagger}\hat{c}_{i+1}\right) + \frac{v}{2}\sum_{i=1}^{N}\hat{n}_i(\hat{n}_i - 1)\right), \tag{2.2}$$

where $v = V/J$ is the relative strenght of the interaction with respect to the hopping energy. Since the evolution of the system is given by the operator $\hat{\mathcal{U}} = \exp(-i\hat{\mathcal{H}}_{BH}t)$, we deduce that J is only a time-dilation factor (which gives the characteristic time of the hopping dynamics of the system J^{-1}), and therefore we should represent the evolution of any physical quantity in the dimensionless time $\tau = |J| \cdot t$, which is equivalent to setting $J = 1$ and using directly t. The only quantity that can change the physics of the system is therefore v.

Bandstructure

The states of the system can be equally represented both in the Fock space and in the symmetrized two-particle Hilbert space, with dimension $N(N+1)/2$ and basis set given by $\{|1,1\rangle_s, |1,2\rangle_s, ..., |2,2\rangle_s, ..., |N,N\rangle_s\}$, where $|i,j\rangle_s$ ($j \geq i$) stands for a symmetrized state in which one particle is localized on site i, and the other on site j. Since the Hubbard Hamiltonian represents the discrete version of the kinetic operator plus a central potential

(depending only on the relative distance among the particles), the dynamics can be factorized in the coordinate space of the center of mass $R = \frac{i+j}{2}$ and the relative distance $r = j - i$, so the ansatz for its eigenfunctions becomes

$$\Psi(R, r) = e^{iKR}\varphi(r), \tag{2.3}$$

and the energy spectrum $E(K) = \omega(K)$ depends on the quasimomentum K, which assumes only discrete values due to the periodic boundary conditions ($K = \frac{2\pi}{N}\nu$, where $\nu = 1, 2, ..., N$).

The explicit derivation of this bandstructure can be found in Ref. [66]. It is composed by a *miniband*, hosting N states with energies near V, and a *main subband*, extendend approximately between $-4J$ and $+4J$ and hosting the remaining $N(N-1)/2$ states[49, 65]. As it is well known, the eigenstates of the miniband are associated with the so-called *bound states*, in which the particles share the same site and show a co-walking dynamics. Conversely, the eigenstates of the main subband, the so-called *scattering states*, have a delocalized wavefunction (with $\varphi(0) \sim 0$) and show a fermionic anti-bunching behaviour in the high V regime [49]. The striking aspect is that also a repulsive potential can create a bound pair of bosons, as it has been shown experimentally [60]. Indeed, the evolution of particles which are initialized in a bound state is dominated by the states of the miniband, which in the high V regime are well separated in energy from the states of the main subband: therefore, the bound-state particles are forced to remain on the same site while performing their quantum walk.

It has been suggested many times [49, 65] that the energy spectrum $\mathrm{Spec}[\mathcal{H}_N(J, V)]$ simply changes its sign when we change the sign of V, i.e. $\mathrm{Spec}[\mathcal{H}_N(J, V)] = -\mathrm{Spec}[\mathcal{H}_N(J, -V)]$ (we consider inverse ordering for the two spectra). For this reasons, it was stated that the dynamics of the system are the same irrespective of the sign of V, as observed in theoretical [49] and experimental works [60].

Hovewer, while this simmetry is always verified for chains with even N, this is not the case for chains with odd N, as it is shown in Fig. 2.1 for $N = 5$, where the two spectra display some clear discrepancies (mostly in the main subband). This differs from what is typically stated in literature [49]. If we refer to the two spectra as $\mathrm{Spec}[\mathcal{H}_N(J, \pm V)] = \{\omega_i^{\pm}\}_i$, then we can define the deviation D_V between them as:

$$D_V(N) = \|\mathrm{Spec}[\mathcal{H}_N(V)] + \mathrm{Spec}[\mathcal{H}_N(-V)]\| = \sqrt{\sum_i \left(\omega_i^+ + \omega_i^-\right)^2}. \tag{2.4}$$

The evolution of D_V against N is reported in Fig. 2.2: as it can be seen, D_V is always zero for even N, while for odd N it goes to zero only in the limit for $N \to \infty$ (as it can be extrapolated from the phenomenological trendline). This suggests that the considered effect is related to differences in periodic boundary conditions, which are less important as soon as N grows.

Our observations on the effects of $\mathrm{sgn}(V)$ over dynamics do not depend on N being even or odd. However, in order to avoid the influence of the asymmetry of the bandstructure, we considered in our simulations only chains with even N. Even in this condition, however, it will be apparent that there are differences in the dynamics when switching from attractive to repulsive interactions (or vice versa).

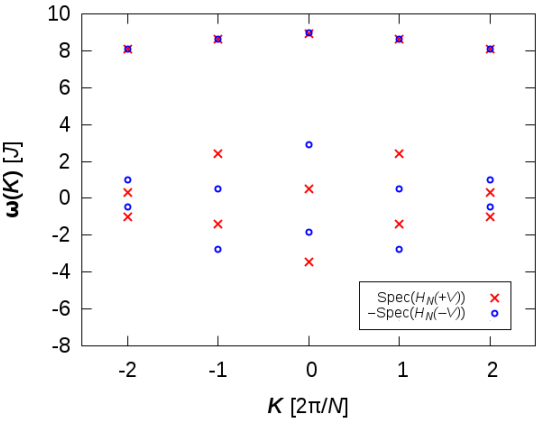

Fig. 2.1 Bandstructure (spectrum) for $\hat{\mathcal{H}}_N(V)$ and $-\hat{\mathcal{H}}_N(-V)$ for $V = 8$ and $N = 5$. Energies are given in units of J, wavevectors in units of $2\pi/N$.

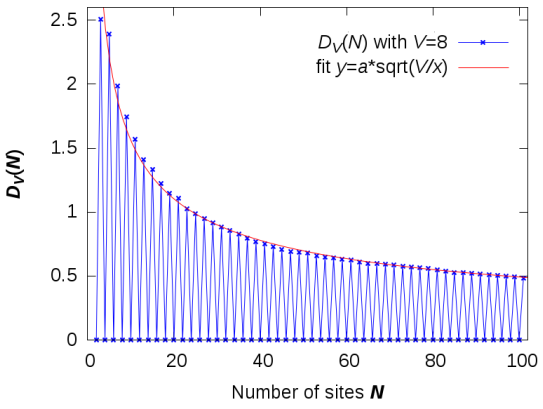

Fig. 2.2 Deviation $D_V(N)$ between the spectra of $\hat{\mathcal{H}}_N(V)$ and $\hat{\mathcal{H}}_N(-V)$ for $V = 8$ at different values of N. The two spectra are exactly opposite ($D_V(N) = 0$) only for even N. The red line is a phenomenological fit for odd N values.

2.2 Quantum Correlations

During the evolution of the system, we can study the particle density

$$n_i(t) = \left\langle \hat{c}_i^\dagger \hat{c}_i \right\rangle \tag{2.5}$$

at each site i of the lattice, and also the two-particle correlation

$$\Gamma_{i,j}(t) = \left\langle \hat{c}_i^\dagger \hat{c}_j^\dagger \hat{c}_j \hat{c}_i \right\rangle \tag{2.6}$$

among sites i and j, which coincides with the diagonal element of the density operator $\rho_{i,j;i,j} =_s \langle i,j|\,\hat{\rho}\,|i,j\rangle_s$ (notice also that $n_i = \sum_i \rho_{i,j;i,j}(1+\delta_{i,j})$). This last quantity is useful to identify behaviours like bunching (or co-walking) and anti-bunching, which depend both on the initial state $|\Psi(0)\rangle$ and on the strenght of the interaction V [49, 55, 56]. In some previous works [49], these correlations have been shown to be independent from the sign of V. Here, we will show that actually they depend on $\mathrm{sgn}(V)$ for some initial states, as it was anticipated in Ref. [38]. For clarity, however, we will graph the normalized two-particle correlations:

$$\tilde{\Gamma}_{i,j}(t) = \frac{\Gamma_{i,j}(t)}{\max\limits_{\{i,j\}}[\Gamma_{i,j}(t)]}. \tag{2.7}$$

Entanglement of Particles

For what concerns the evaluation of the entanglement among the walkers, following our previous work [38] we adopt the formalism of the *entanglement of particles*, defined by Wiseman and Vaccaro[24]. In this approach, the modes of the system (i.e., the sites), are divided into two groups: one controlled by Alice, and one controlled by Bob. We choose a geometrical partition in which the first half of the lattice, namely sites $A = \{1, 2, ..., \frac{N}{2}\}$, is controlled by Alice, while the remaining sites $B = \{\frac{N}{2}+1, ..., N\}$ are controlled by Bob. Each subsystem has a set of standard quantum registers, i.e. a set of distinguishable qubits, in addition to the indistinguishable particles described by the state $\rho_{AB} = \hat{\rho}(t)$. By means of local operations on the modes they control, Alice and Bob can transfer a certain amount of entanglement to their standard quantum registers, and the maximum amount of such entanglement gives the *entanglement of particles* E_P. However, in order to produce physically exploitable correlations, these local operations must not violate the *superselection rule* of the *local particle number*. Therefore, Alice and Bob must possess each one a definite number of particles. Then, for a system with a total number of particles n, the entanglement E_P is given by:

$$E_P = \sum_{k=0}^{n} P_{k,n-k}\mathcal{E}(\rho_{k,n-k}), \tag{2.8}$$

where

$$\rho_{k,n-k} = \Pi_{k,n-k}\rho\Pi_{k,n-k} \tag{2.9}$$

is the projection of the system state ρ over the subspace in which A possesses exactly k particles and B the remaining $n-k$ ones, while $P_{k,n-k} = \mathrm{Tr}_{AB}[\rho_{k,n-k}]$ is the corresponding probability. For any bipartition $A = \{n_{Ai}\}_i$ and $B = \{n_{Bi}\}_i$, the projector $\Pi_{k,n-k}$ is given by:

$$\begin{aligned}\Pi_{k,n-k} &= \sum_{\substack{\Sigma_i n_{Ai}=k \\ \Sigma_i n_{Bi}=n-k}} |\{n_{Ai}\}\{n_{Bi}\}\rangle\langle\{n_{Ai}\}\{n_{Bi}\}|\,, \\ &= \left(\sum_{\Sigma_i n_{Ai}=k} |\{n_{Ai}\}\rangle\langle\{n_{Ai}\}|\right) \otimes \left(\sum_{\Sigma_i n_{Bi}=n-k} |\{n_{Bi}\}\rangle\langle\{n_{Bi}\}|\right),\end{aligned} \tag{2.10}$$

and the completeness relation gives:

$$\sum_{k=0}^{n} \Pi_{k,n-k} = I. \tag{2.11}$$

The quantity $\mathcal{E}$ can be any standard measure of bipartite entanglement among the registers of Alice and Bob (*entanglement of modes*). For our two-particle system, situations where $k = 0$ or $k = 2$ give zero correlations $\mathcal{E} = 0$, therefore Eq. (2.8) reduces to

$$E_P = P_{1,1}\mathcal{E}(\rho_{1,1}). \tag{2.12}$$

Since we are considering a noiseless system, where the states remain pure during all their evolution, we can use for $\mathcal{E}(\rho_{AB})$ ($\rho_{AB} = \rho_{1,1}$) the *linear entropy*[19]

$$\mathcal{E}(\rho_{AB}) = \frac{N/2}{N/2-1}\left(1 - \mathrm{Tr}_A[\rho_A^2]\right), \tag{2.13}$$

where $\rho_A = \mathrm{Tr}_B[\rho_{AB}]/\mathrm{Tr}_{AB}[\rho_{AB}]$ is the reduced density matrix of the subsystem A. Anyway, equivalent results (not shown in the paper) can be obtained with the *von Neumann entropy*

$$\mathcal{E}(\rho_{AB}) = -\frac{1}{\ln(N/2)}\mathrm{Tr}_A[\rho_A \ln \rho_A], \tag{2.14}$$

or the *Negativity*

$$\mathcal{E}(\rho_{AB}) = \frac{1}{N/2-1}\left(\left\|\tilde{\rho}_{AB}^{T_B}\right\|_1 - 1\right), \tag{2.15}$$

which is defined as the sum of the negative eigenvalues of $\tilde{\rho}_{AB}^{T_B}$ (the partial transpose of $\rho_{AB}/\mathrm{Tr}_{AB}[\rho_{AB}]$ with respect to the subsystem B) and renormalized to 1 for a maximally entangled state[67, 68] ($\|\cdot\|_1$ is the so-called *trace norm,* which is given by the sum of the eigenvalues).
It is worth noting that E_P depends upon the chosen bipartition of the system modes among Alice and Bob: therefore, different partitions of the system can lead to different values of E_P. Also, it should be mentioned that E_P does not capture all the quantum correlations encoded in the system: indeed, "ideal" co-walking situations, where the particles are strongly correlated, do not give contributions to E_P (since they correspond to $k = 0$ or $k = 2$), but actually those states cannot be exploited to perform quantum computing tasks, since one of the two observers is left with no particle on wich he or she can perform any local operation.

3 Quantum Walk Simulation

As a representative situation, we choose for our calculations a lattice with $N = 30$ sites. The dynamics of the system is driven alternatively by the hamiltonians $\hat{\mathcal{H}}_+ = \hat{\mathcal{H}}_N(J, V)$ and $\hat{\mathcal{H}}_- = \hat{\mathcal{H}}_N(J, -V)$, where $J = 1$ and $V = 8$. Their spectra $\omega(K)$ (which are symmetrical with respect to $\omega = 0$) are reported in Fig. 3.1
Through the numerical diagonalization of the Hamiltonian of Eq. (2.1), we can build the evolution operator $\hat{\mathcal{U}}(t) = \exp(-i\hat{\mathcal{H}}_{BH}t)$ of the system for any time t. Therefore, given the initial state $\hat{\rho}(0) = |\Psi(0)\rangle\langle\Psi(0)|$, the state at time t is given by

$$\hat{\rho}(t) = \hat{\mathcal{U}}(t)\hat{\rho}(0)\hat{\mathcal{U}}^\dagger(t). \tag{3.1}$$

We choose as initial states $|\Psi(0)\rangle$ the following ones:

$$|\Psi_1\rangle = |15, 17\rangle_s, \tag{3.2}$$
$$|\Psi_2\rangle = |14, 16\rangle_s, \tag{3.3}$$
$$|\Psi_3\rangle = |14, 17\rangle_s, \tag{3.4}$$
$$|\Psi_4\rangle = |14, 16\rangle_s + |15, 17\rangle_s, \tag{3.5}$$
$$|\Psi_5\rangle = |14, 16\rangle_s + |14, 17\rangle_s, \tag{3.6}$$

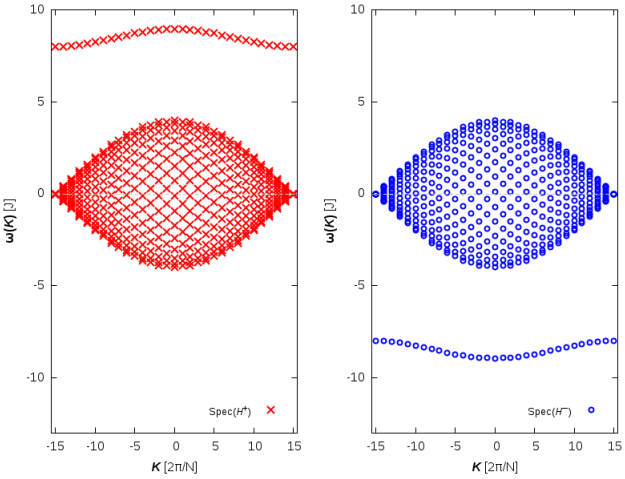

Fig. 3.1 Bandstructure $\omega(K)$ of a chain with $N = 30$ sites at $V/J = +8$ (left, red) and $V/J = -8$ (right, blue).

which we evolve, alternatively, under the action of $\hat{\mathcal{U}}_+(t)$ ($\hat{\mathcal{H}}_+$) and $\hat{\mathcal{U}}_-(t)$ ($\hat{\mathcal{H}}_-$).
In our calculations, we considered only times t at wich the wavefunction $|\Psi(t)\rangle$ of the particles is far from the boundaries of the lattice, in order to avoid interference effects due to periodic boundary conditions.
As it can be seen in Figure 3.2, the correlations $\tilde{\Gamma}_{i,j}$ of the states $|\Psi_1\rangle$, $|\Psi_2\rangle$ and $|\Psi_3\rangle$ are invariant under the sign exchange of V. Here calculations are performed with $V = \pm 8$, but a large number of simulations with different values of V has shown qualitatively identical behaviours. Notice that the evolutions of $|\Psi_1\rangle$ and $|\Psi_2\rangle$ are practically identical, except for a rigid shift, and this is perfectly reasonable since $\hat{\mathcal{H}}_N$ with periodic boundary conditions commutes with the translation operator $\hat{T}_l = \Sigma_i |i + l\rangle\langle i|$, therefore two states that differ only for a rigid shift of $l = 1$ sites ($|\Psi_1\rangle = \hat{T}_1 |\Psi_2\rangle$) must have the same dynamics. The same behaviour is found for the entanglement of particles, which is identical both for $\hat{\mathcal{H}}_+$ and $\hat{\mathcal{H}}_-$ and is reported in Fig. 3.4 (the entanglement is initially zero since all states are symmetrized versions of factorizable states).

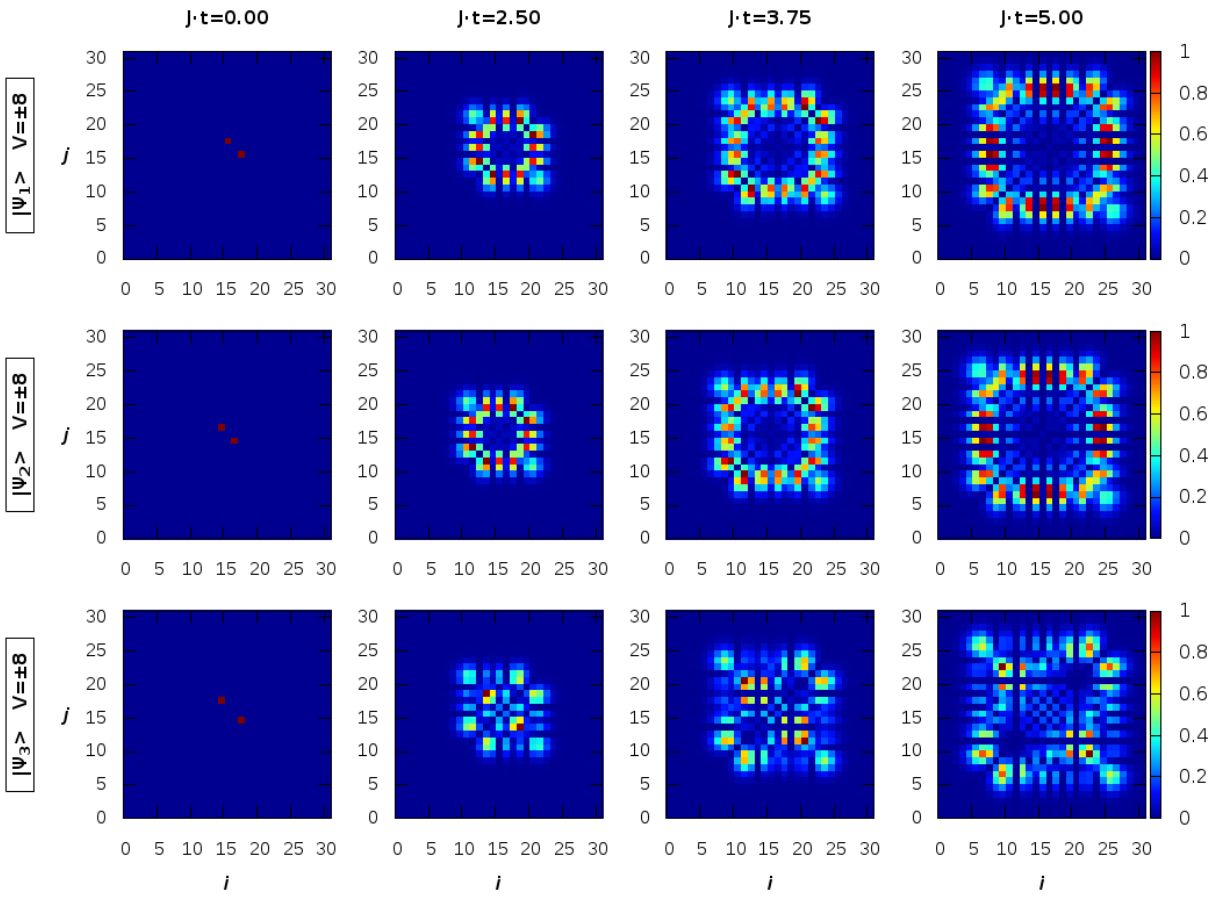

Fig. 3.2 Evolution of two-sites correlations $\tilde{\Gamma}_{i,j}$ in states $|\Psi_1\rangle, |\Psi_2\rangle$ and $|\Psi_3\rangle$ under $\hat{\mathcal{H}}_+$ and $\hat{\mathcal{H}}_-$, with $V = \pm 8$ and $J = 1$.

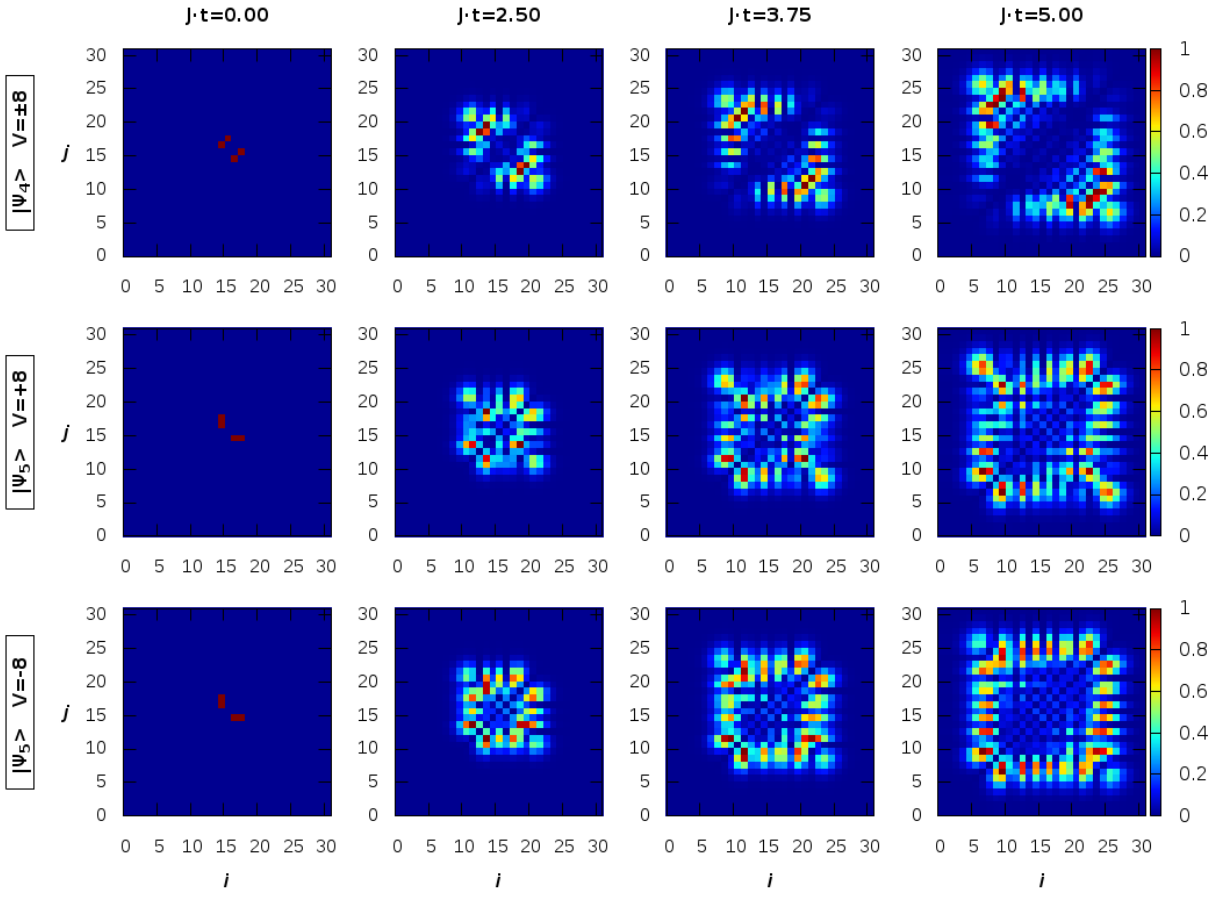

Fig. 3.3 Evolution of two-sites correlations $\tilde{\Gamma}_{i,j}$ in states $|\Psi_4\rangle$ and $|\Psi_5\rangle$ under $\hat{\mathcal{H}}_+$ and $\hat{\mathcal{H}}_-$. Parameters are the same as in Fig.3.2.

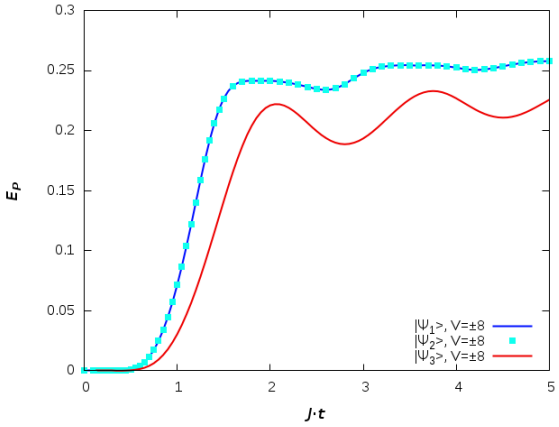

Fig. 3.4 Evolution of entanglement of particles in states $|\Psi_1\rangle, |\Psi_2\rangle$ and $|\Psi_3\rangle$ under $\hat{\mathcal{H}}_{\pm}$.

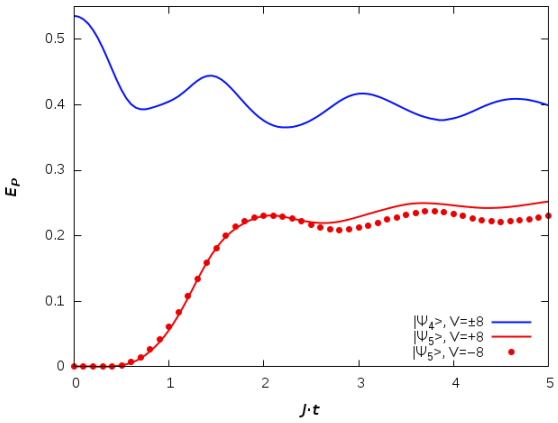

Fig. 3.5 Evolution of Entanglement of particles in states $|\Psi_4\rangle$ and $|\Psi_5\rangle$ under $\hat{\mathcal{H}}_{\pm}$.

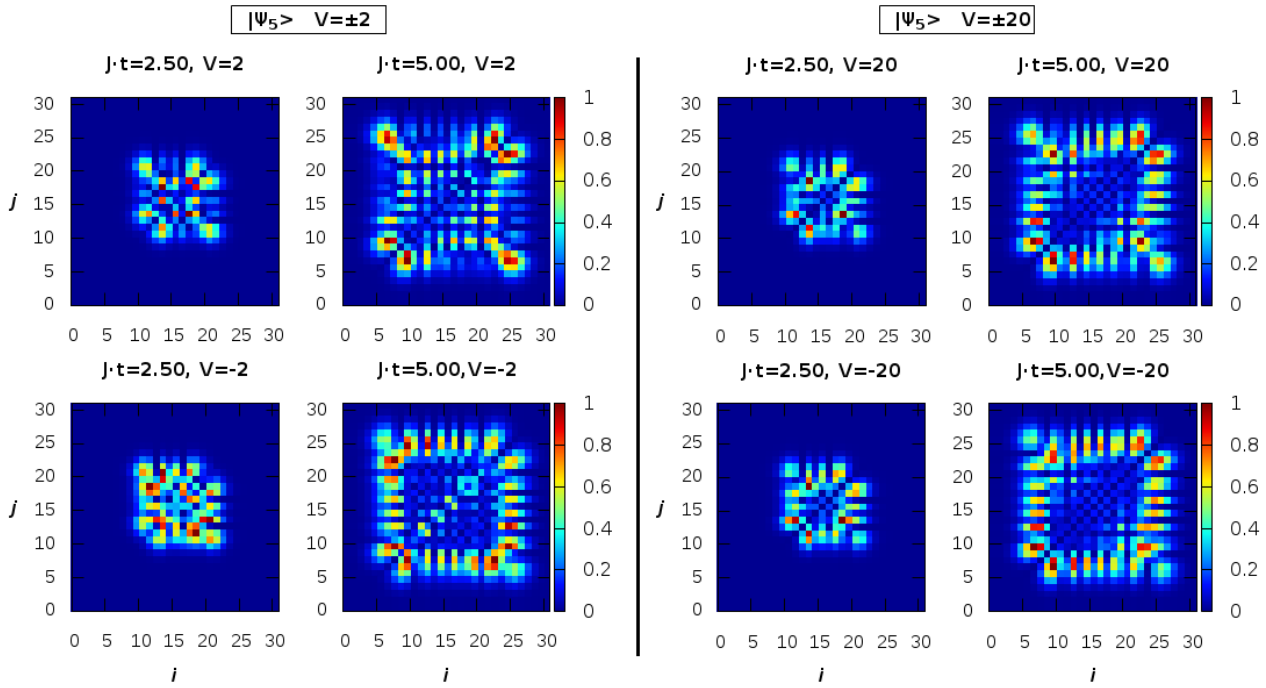

Fig. 3.6 Evolution of two-sites correlations $\tilde{\Gamma}_{i,j}$ in state $|\Psi_5\rangle$ under $\hat{\mathcal{H}}_+$ and $\hat{\mathcal{H}}_-$ for different values of V and for $J = 1$. Differences between evolutions are more apparent at low potential energies (i.e. $V \sim J$)

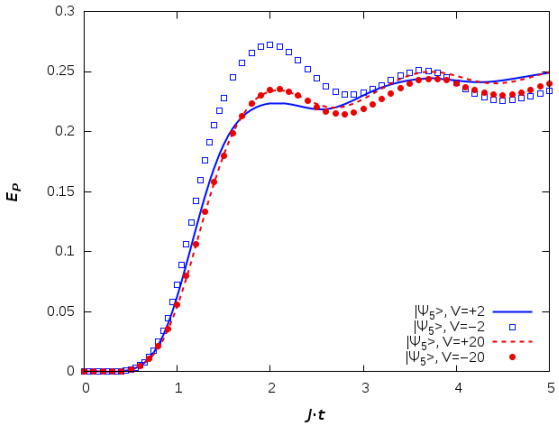

Fig. 3.7 Evolution of Entanglement E_P in states $|\Psi_5\rangle$ under $\hat{\mathcal{H}}_{\pm}$ for different values of V.

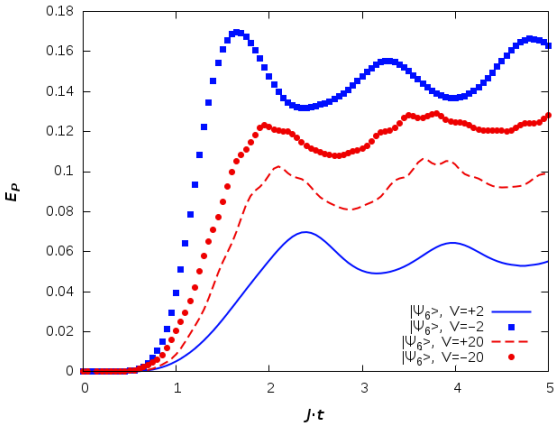

Fig. 3.8 Evolution of Entanglement E_P in state $|\Psi_6\rangle$ under $\hat{\mathcal{H}}_{\pm}$.

Notice that the initial states here considered ($|\Psi_1\rangle$, $|\Psi_2\rangle$ and $|\Psi_3\rangle$) are eigenstates of the number operators $\hat{n}_i$, i.e. they have an exact number of particles in each site of the lattice. As it was already observed by Lahini et al. [49], the evolution of these states is invariant when switching from $\hat{\mathcal{H}}_+$ to $\hat{\mathcal{H}}_-$. However, the same consideration does not hold, in general, for superpositions of these states: indeed, as it can be seen in Fig. 3.3, the evolution of correlations $\Gamma_{i,j}$ in $|\Psi_4\rangle$ is the same for V and $-V$, whereas the evolution of correlations in $|\Psi_5\rangle$ is appreciably different for attractive and repulsive interactions. The same signatures of the interaction potential can be seen in the entanglement of particles (Fig. 3.5): the entanglement of state $|\Psi_4\rangle$ is independent from the sign of V, while the entanglement of$|\Psi_5\rangle$ is different for V and $-V$ (notice that $E_P(|\Psi_5\rangle)$ is initially 0 since the state is factorizable).
Surprinsingly, further explorations show that this effect is more marked at a lower interaction energy: in Fig. 3.6, we see that differences in $\tilde{\Gamma}_{i,j}$ for $|\Psi_5\rangle$ are more marked at $V = \pm 2$ than at $V = \pm 20$, and the same behaviour is found for entanglement (see Fig. 3.7). Indeed, for some states, e.g.

$$|\Psi_6\rangle = |14, 14\rangle_s + |14, 17\rangle_s \,, \tag{3.7}$$

at low interaction energy $V/J = \pm 2$ we can observe a difference of a factor larger than 2 in the entanglement of particles (see Fig. 3.8).

4 Discussion

In order to understand the behaviour of the system, we realize an analytical toy-model of a chain with $N = 4$ sites.
In Fig. 4.1 it is represented the bandstructure (a) of $\hat{\mathcal{H}}_+ = \hat{\mathcal{H}}_4(J, V)$ and $\hat{\mathcal{H}}_- = \hat{\mathcal{H}}_4(J, -V)$ (as before, $J = 1$ and $V = 8$), together with the evolution (b) of the eigenvalues of $\hat{\mathcal{H}}_+$ with increasing V. The eigenvalues of $\hat{\mathcal{H}}_+$ are called ω_i^+ and are listed in Table 1, while the eigenvalues of $\hat{\mathcal{H}}_-$ can be obtained analytically from the relation $\omega_i^- = -\omega_i^+$, as it can bee seen also from Table 1 with the substitution $V \to -V$ and in Fig. 4.1.a from numerical diagonalization. However, since the system is invariant under time-reversal, any change in the dynamics cannot be related to the simple sign switching of the eigenvalues.

		Eigenvalue	Degen.
Miniband	ω_1^+	$\frac{V}{3} + \frac{48J^2+V^2}{9\gamma} + \gamma$	1
	$\omega_{2,3}^+$	$\frac{V+\sqrt{16J^2+V^2}}{2}$	2
	ω_4^+	V	1
Main subband	ω_5^+	$V + \omega_1^+(J,-V) - \omega_1^+(J,V) = \frac{V}{3} + \left(\frac{48J^2+V^2}{9\gamma\gamma'} - 1\right)(\gamma - \gamma')$	1
	$\omega_{6,7}^+$	$\frac{V-\sqrt{16J^2+V^2}}{2}$	2
	$\omega_{8,9}^+$	0	2
	ω_{10}^+	$-\omega_1^+(J,-V) = \frac{V}{3} - \frac{48J^2+V^2}{9\gamma'} - \gamma'$	1
$\gamma(J,V) = \left(\sqrt{\left(\frac{4J^2V}{3} - \frac{V^3}{27}\right)^2 - \left(\frac{16J^2}{3} + \frac{V^2}{9}\right)^3} - \frac{4J^2V}{3} + \frac{V^3}{27}\right)^{\frac{1}{3}}$			$\gamma' = \gamma(J,-V)$

Table 1 Eigenvalues of $\hat{\mathcal{H}}_+$ with relative multiplicity (degeneracy), ordered by decreasing energy.

The eigenfunctions $\Psi_i^{\pm}(R, r) = exp(iKR)\varphi_i^{\pm}(r)$ are described by Eq. (2.3). As it was shown in Ref. [65], their radial parts $\varphi_i^{\pm}(r)$ change sign in some components when switching from $\hat{\mathcal{H}}_+$ to $\hat{\mathcal{H}}_-$, while others remain completely unchanged, but in any case their squared modulus remains unchanged (see Fig 4.1.c for comparison). This suggests that the different behaviours with attractive/repulsive interactions depend on this feature of the eigenstates.
For what concerns the number eigenstates, due to the translational invariance of the chain, the only states which are physically different are $|1, 1\rangle_s$, $|1, 2\rangle_s$ and $|1, 3\rangle_s$. Each of these states can be decomposed on the eigenstates of the hamiltonian, leading to

$$|j, k\rangle_s = \sum_i C_{j,k,i}^{\pm} \left|\Psi_i^{\pm}\right\rangle . \tag{4.1}$$

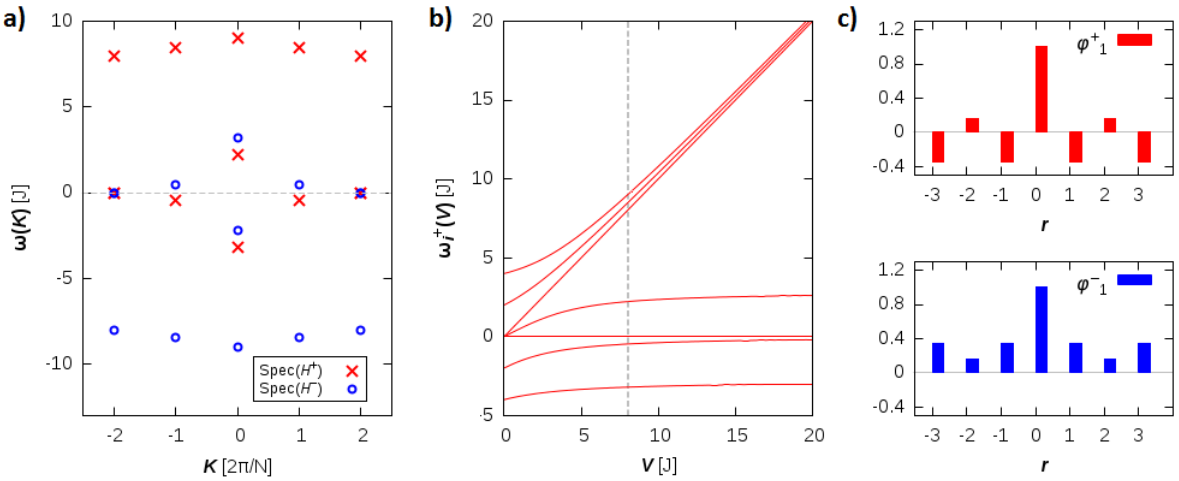

Fig. 4.1 **a)** Bandstructures for $\hat{\mathcal{H}}_+$ (red crosses) and $\hat{\mathcal{H}}_-$ (blue dots) at $V = \pm 8$. The main subband and the miniband are clearly visible, as well as the symmetry of the two spectra. **b)** Evolution of the eigenvalues ω_i^+ at increasing V: for high values of the potential energy, there is a clear separation between the miniband (which becomes almost flat) and the main subband, while at low V the two subbands are entwined. The grey vertical dashed line indicates $V = 8$ (subfig. a). **c)** Radial wavefunction for the first eigenstate of $\hat{\mathcal{H}}_+$ (upper, red) and $\hat{\mathcal{H}}_-$(lower, blue).

Since the hamiltonians $\hat{\mathcal{H}}_\pm$ are real, it is always possible to choose a set of eigenstates $|\Psi_i^\pm\rangle$ having real components in the number states basis, therefore the scalar products

$$C^\pm_{j,k,i} = \langle \Psi_i^\pm | j,k \rangle_s \tag{4.2}$$

that we obtain with the projection are real numbers too.

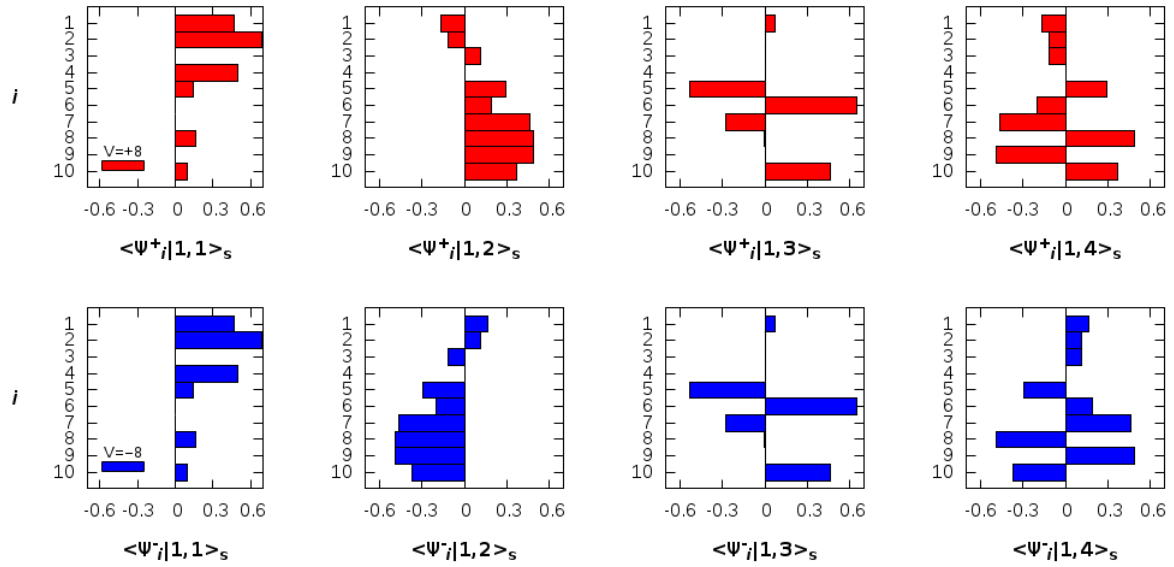

Fig. 4.2 Projections of number states $|1,1\rangle_s$, $|1,2\rangle_s$, $|1,3\rangle_s$ and $|1,4\rangle_s$ over the eigenstates of $\hat{\mathcal{H}}_+$ (first row, red) and $\hat{\mathcal{H}}_-$ (second row, blue) for a potential energy of $|V| = 8$. Notice that, as expected, $|1,4\rangle_s$ behaves like $|1,2\rangle_s$, and their projections are also identical in modulus (since the two states are translationally equivalent).

As you can see in Figure 4.2, all the projections of states like $|1,1\rangle_s$ and $|1,3\rangle_s$ do not change sign when we switch from $\hat{\mathcal{H}}_+$ to $\hat{\mathcal{H}}_-$, while the projections of states like $|1,2\rangle_s$ do change all their signs. This is the reason why superpositions of (translationally) equivalent number eigenstates, like

$$|\Psi_B\rangle = |1,3\rangle_s + |2,4\rangle_s\,, \tag{4.3}$$

have the same correlations and entanglement indepdently from the sign of V, while superpositions of non-equivalent number eigenstates, like

$$|\Xi_B\rangle = |1,4\rangle_s + |2,4\rangle_s\,, \tag{4.4}$$

have a different evolution of their correlations under $\hat{\mathcal{H}}_+$ and $\hat{\mathcal{H}}_-$, as it was shown in Ref. [38]. Indeed, the change of sign in V introduces a relative phase between the components of the two number eigenstates, which is different for $\hat{\mathcal{H}}_+$ and $\hat{\mathcal{H}}_-$, thus leading to different evolutions of the states. As an example, we have

$$\hat{\mathcal{U}}(t)\left(|1,3\rangle_s + |2,4\rangle_s\right) = \begin{cases} \sum_i \left(C^+_{1,3,i} + C^+_{2,4,i}\right)|\Psi^+_i(t)\rangle & V > 0, \\ \sum_i \left(C^+_{1,3,i} + C^+_{2,4,i}\right)|\Psi^-_i(t)\rangle & V < 0, \end{cases} \tag{4.5}$$

$$\hat{\mathcal{U}}(t)\left(|1,4\rangle_s + |2,4\rangle_s\right) = \begin{cases} \sum_i \left(C^+_{1,4,i} + C^+_{2,4,i}\right)|\Psi^+_i(t)\rangle & V > 0, \\ \sum_i \left(-C^+_{1,4,i} + C^+_{2,4,i}\right)|\Psi^-_i(t)\rangle & V < 0. \end{cases} \tag{4.6}$$

It must be stressed now that the coefficients $C^{\pm}_{j,k,i}$ can only change sing when we change the sign of V, therefore we cannot observe this effect directly when we study a single number eigenstate (e.g., by setting $|\Psi(0)\rangle = |1,3\rangle_s$), because the squared modulus of the projections do not depend on $\mathrm{sgn}(C^{\pm}_{j,k,i})$. Only superpositions of number eigenstates can show the signature of the nature of the interaction potential. This is the reason for which previous works in the literature [49] did not observe this dependence.
Indeed, going back to our calculations on the 1D chain with $N = 30$, we notice that states like $|\Psi_1\rangle$ and $|\Psi_2\rangle$ are of the same kind, i.e. second nearest-neighbours like $|i, i+2\rangle_s$ (this is the reason why they show the same evolution of two-site correlations - except for a rigid translation), while the state $|\Psi_3\rangle$ is a third nearest-neighbour state, like $|i, i+3\rangle_s$. This is the reason why $|\Psi_1\rangle$ and $|\Psi_2\rangle$ have equal projections on the eigenstates of $\mathcal{H}_\pm$, whereas the projections of $|\Psi_3\rangle$ are different. Therefore, the linear combination of $|\Psi_1\rangle$ and $|\Psi_2\rangle$ is invariant under the exchange of $\mathrm{sgn}(V)$, while the linear combination of $|\Psi_2\rangle$ and $|\Psi_3\rangle$ is not (some projections exchange sign for a state but not for the other).
For what concerns the behaviour of a state like $|\Psi_6\rangle$, the effect of switching the sign of V is more marked at low potential energy because for $V \sim J$ the main subband and the miniband are strongly mixed, therefore each number eigenstate has a projection over all the eigenvectors of $\hat{\mathcal{H}}_\pm$, and states with different nature have therefore very different superpositions under $\hat{\mathcal{H}}_+$ and $\hat{\mathcal{H}}_-$. On the contrary, for high values of V/J the entanglement shows a less marked difference due to the strong separation between the subband and the miniband (see Fig. 4.1.b). Indeed, this separation implies that the projections of the bound state $|14,14\rangle_s$ are almost completely contained in the miniband, while the ones of the scattering state $|14,17\rangle_s$ are mainly in the main subband. Therefore, the couples $C^{\pm}_{14,14,i} + C^{\pm}_{14,17,i}$ do not change significantly their (absolute) values when switching from $\hat{\mathcal{H}}_+$ to $\hat{\mathcal{H}}_-$ since, for each i, only one coefficient in the sum is significantly different from zero. A similar behaviour can be assumed for $|\Psi_5\rangle$, which is composed by the scattering states $|14,16\rangle_s$ and $|14,17\rangle_s$, both belonging to the main subband: if at higher V these states have their most significant projections mainly over different eigenstates of the main subband, we do not expect to see a very marked change in the entanglement when switching from attractive to repulsive interactions (or vice versa), as we see in Fig. 3.8.

5 Conclusions

In this paper we have shown that in the Bose-Hubbard model both two-sites correlations and entanglement of particles are differently affected by on-site attractive and repulsive interactions. Surprisingly, these differences are more significant for "low" values of the interaction potential V, i.e. of the order of the hopping amplitude J, thus allowing for an easier experimental implementation using actual technologies [60, 61]. This behaviour arises from the fact that the projections of some number states (on the eigenfunctions of the Hubbard model) can change sign when we change the sign of V. Therefore, the effect of $\mathrm{sgn}(V)$ can be observed only with linear combinations of number states that have projections with a different behaviour. This explains why this feature has not been observed before, since most of the present literature is manly focused on the study of a single number state.
The dependence of correlations upon the sign of V can be very marked, even up to a factor 2, as we have seen for entanglement. Such phenomenon provides us a further degree of freedom for manipulating the correlations in a quantum walk, and therefore we think it could be exploited in the next future for performing specific quantum computing tasks.
As a further perspective of research, it would be interesting to study whether this behaviour can be replied in the Fermi-Hubbard model (with spin-$\frac{1}{2}$ electrons) or if it is an exclusive feature of bosons, since some experimental and theoretical works in the literature [58, 69, 70] suggested that the behaviour of Hubbard fermions is the same irrespective of the sign of V. In contrast, some recent works [71] evidence a breaking of the symmetry $\pm V$ for long-range hopping in hard-core bosons. Therefore, it seems worth for us to explore the signatures of long-range hopping and interactions (i.e., extended to first- and second-nearest neighbouring sites) on the dynamics and the entanglement of both bosonic and fermionic particles.

Acknowledgements This work has been supported by UniMORE through FAR2014. We thank Ilaria Siloi for fruitful discussions.

References

1. J. Kempe, "Quantum random walks: An introductory overview," *Contemporary Physics*, vol. 44, no. 4, pp. 307–327, 2003. [Online]. Available: http://dx.doi.org/10.1080/0010715103100011077 6
2. S. Venegas-Andraca, "Quantum walks: a comprehensive review," *Quantum Information Processing*, vol. 11, no. 5, pp. 1015–1106, 2012. [Online]. Available: http://dx.doi.org/10.1007/s11128-012-0432-5
3. A. Ambainis, "Quantum walks and their algorithmic applications," *International Journal of Quantum Information*, vol. 01, no. 04, pp. 507–518, 2003. [Online]. Available: http://www.worldscientific.com/doi/abs/10.1142/S0219749903000383
4. R. Portugal, *Quantum walks and search algorithms*. Springer Science & Business Media, 2013.
5. S. E. Venegas-Andraca, "Quantum walks for computer scientists," *Synthesis Lectures on Quantum Computing*, vol. 1, no. 1, pp. 1–119, 2008.
6. Y. Bromberg, Y. Lahini, R. Morandotti, and Y. Silberberg, "Quantum and classical correlations in waveguide lattices," *Phys. Rev. Lett.*, vol. 102, p. 253904, Jun 2009. [Online]. Available: http://link.aps.org/doi/10.1103/PhysRevLett.102.253904
7. A. Peruzzo, M. Lobino, J. C. F. Matthews, N. Matsuda, A. Politi, K. Poulios, X.-Q. Zhou, Y. Lahini, N. Ismail, K. Wörhoff, Y. Bromberg, Y. Silberberg, M. G. Thompson, and J. L. OBrien, "Quantum walks of correlated photons," *Science*, vol. 329, no. 5998, pp. 1500–1503, 2010.
8. A. Rai, G. S. Agarwal, and J. H. H. Perk, "Transport and quantum walk of nonclassical light in coupled waveguides," *Phys. Rev. A*, vol. 78, p. 042304, Oct 2008. [Online]. Available: http://link.aps.org/doi/10.1103/PhysRevA.78.042304
9. J. Wang and K. Manouchehri, *Physical implementation of quantum walks*. Springer, 2013.
10. M. A. Broome, A. Fedrizzi, S. Rahimi-Keshari, J. Dove, S. Aaronson, T. C. Ralph, and A. G. White, "Photonic boson sampling in a tunable circuit," *Science*, vol. 339, no. 6121, pp. 794–798, 2013.
11. J. B. Spring, B. J. Metcalf, P. C. Humphreys, W. S. Kolthammer, X.-M. Jin, M. Barbieri, A. Datta, N. Thomas-Peter, N. K. Langford, D. Kundys, J. C. Gates, B. J. Smith, P. G. R. Smith, and I. A. Walmsley, "Boson sampling on a photonic chip," *Science*, vol. 339, no. 6121, pp. 798–801, 2013. [Online]. Available: http://www.sciencemag.org/content/339/6121/798.abstract
12. M. Tillmann, B. Dakić, R. Heilmann, S. Nolte, A. Szameit, and P. Walther, "Experimental boson sampling," *Nature Photonics*, vol. 7, no. 7, pp. 540–544, 2013.
13. J. D. Franson, "Beating classical computing without a quantum computer," *Science*, vol. 339, no. 6121, pp. 767–768, 2013. [Online]. Available: http://www.sciencemag.org/content/339/6121/767.short
14. C. Benedetti, F. Buscemi, and P. Bordone, "Quantum correlations in continuous-time quantum walks of two indistinguishable particles," *Phys. Rev. A*, vol. 85, p. 042314, Apr 2012. [Online]. Available: http://link.aps.org/doi/10.1103/PhysRevA.85.042314
15. K. Mayer, M. C. Tichy, F. Mintert, T. Konrad, and A. Buchleitner, "Counting statistics of many-particle quantum walks," *Phys. Rev. A*, vol. 83, p. 062307, Jun 2011. [Online]. Available: http://link.aps.org/doi/10.1103/PhysRevA.83.062307
16. J. Schliemann, J. I. Cirac, M. Kuś, M. Lewenstein, and D. Loss, "Quantum correlations in two-fermion systems," *Phys. Rev. A*, vol. 64, p. 022303, Jul 2001. [Online]. Available: http://link.aps.org/doi/10.1103/PhysRevA.64.022303
17. K. Eckert, J. Schliemann, D. Bruß, and M. Lewenstein, "Quantum correlations in systems of indistinguishable particles," *Annals of Physics*, vol. 299, no. 1, pp. 88 – 127, 2002. [Online]. Available: http://www.sciencedirect.com/science/article/pii/S0003491602962688
18. F. Buscemi, P. Bordone, and A. Bertoni, "Entanglement dynamics of electron-electron scattering in low-dimensional semiconductor systems," *Phys. Rev. A*, vol. 73, p. 052312, May 2006. [Online]. Available: http://link.aps.org/doi/10.1103/PhysRevA.73.052312
19. ——, "Linear entropy as an entanglement measure in two-fermion systems," *Phys. Rev. A*, vol. 75, p. 032301, Mar 2007. [Online]. Available: http://link.aps.org/doi/10.1103/PhysRevA.75.032301
20. P. Zanardi, "Quantum entanglement in fermionic lattices," *Phys. Rev. A*, vol. 65, p. 042101, Mar 2002. [Online]. Available: http://link.aps.org/doi/10.1103/PhysRevA.65.042101
21. G. C. Ghirardi, L. Marinatto, and T. Weber, "Entanglement and properties of composite quantum systems: A conceptual and mathematical analysis," *Journal of Statistical Physics*, vol. 108, no. 1-2, pp. 49–122, 2002. [Online]. Available: http://dx.doi.org/10.1023/A%3A1015439502289
22. G. C. Ghirardi and L. Marinatto, "General criterion for the entanglement of two indistinguishable particles," *Phys. Rev. A*, vol. 70, p. 012109, Jul 2004. [Online]. Available: http://link.aps.org/doi/10.1103/PhysRevA.70.012109
23. F. Benatti, R. Floreanini, and K. Titimbo, "Entanglement of identical particles," *Open Systems & Information Dynamics*, vol. 21, no. 01n02, p. 1440003, 2014. [Online]. Available: http://www.worldscientific.com/doi/abs/10.1142/S1230161214400034

24. H. M. Wiseman and J. A. Vaccaro, "Entanglement of indistinguishable particles shared between two parties," *Phys. Rev. Lett.*, vol. 91, p. 097902, Aug 2003. [Online]. Available: http://link.aps.org/doi/10.1103/PhysRevLett.91.097902
25. M. R. Dowling, A. C. Doherty, and H. M. Wiseman, "Entanglement of indistinguishable particles in condensed-matter physics," *Phys. Rev. A*, vol. 73, p. 052323, May 2006. [Online]. Available: http://link.aps.org/doi/10.1103/PhysRevA.73.052323
26. T. Sasaki, T. Ichikawa, and I. Tsutsui, "Entanglement of indistinguishable particles," *Phys. Rev. A*, vol. 83, p. 012113, Jan 2011. [Online]. Available: http://link.aps.org/doi/10.1103/PhysRevA.83.012113
27. F. Iemini, T. Maciel, T. Debarba, and R. Vianna, "Quantifying quantum correlations in fermionic systems using witness operators," *Quantum Information Processing*, vol. 12, no. 2, pp. 733–746, 2013. [Online]. Available: http://dx.doi.org/10.1007/s11128-012-0415-6
28. F. Iemini and R. O. Vianna, "Computable measures for the entanglement of indistinguishable particles," *Phys. Rev. A*, vol. 87, p. 022327, Feb 2013. [Online]. Available: http://link.aps.org/doi/10.1103/PhysRevA.87.022327
29. F. Iemini, T. Debarba, and R. O. Vianna, "Quantumness of correlations in indistinguishable particles," *Phys. Rev. A*, vol. 89, p. 032324, Mar 2014. [Online]. Available: http://link.aps.org/doi/10.1103/PhysRevA.89.032324
30. A. Reusch, J. Sperling, and W. Vogel, "Entanglement witnesses for indistinguishable particles," *Phys. Rev. A*, vol. 91, p. 042324, Apr 2015. [Online]. Available: http://link.aps.org/doi/10.1103/PhysRevA.91.042324
31. P. Zanardi, D. A. Lidar, and S. Lloyd, "Quantum tensor product structures are observable induced," *Phys. Rev. Lett.*, vol. 92, p. 060402, Feb 2004. [Online]. Available: http://link.aps.org/doi/10.1103/PhysRevLett.92.060402
32. H. Barnum, E. Knill, G. Ortiz, R. Somma, and L. Viola, "A subsystem-independent generalization of entanglement," *Phys. Rev. Lett.*, vol. 92, p. 107902, Mar 2004. [Online]. Available: http://link.aps.org/doi/10.1103/PhysRevLett.92.107902
33. F. Benatti, R. Floreanini, and U. Marzolino, "Entanglement robustness and geometry in systems of identical particles," *Phys. Rev. A*, vol. 85, p. 042329, Apr 2012. [Online]. Available: http://link.aps.org/doi/10.1103/PhysRevA.85.042329
34. ——, "Entanglement in fermion systems and quantum metrology," *Phys. Rev. A*, vol. 89, p. 032326, Mar 2014. [Online]. Available: http://link.aps.org/doi/10.1103/PhysRevA.89.032326
35. L. Mazza, D. Rossini, R. Fazio, and M. Endres, "Detecting two-site spin-entanglement in many-body systems with local particle-number fluctuations," *New Journal of Physics*, vol. 17, no. 1, p. 013015. [Online]. Available: http://stacks.iop.org/1367-2630/17/i=1/a=013015
36. F. Iemini, T. O. Maciel, and R. O. Vianna, "Entanglement of indistinguishable particles as a probe for quantum phase transitions in the extended hubbard model," *Phys. Rev. B*, vol. 92, p. 075423, Aug 2015. [Online]. Available: http://link.aps.org/doi/10.1103/PhysRevB.92.075423
37. F. Buscemi and P. Bordone, "Measure of tripartite entanglement in bosonic and fermionic systems," *Phys. Rev. A*, vol. 84, p. 022303, Aug 2011. [Online]. Available: http://link.aps.org/doi/10.1103/PhysRevA.84.022303
38. A. Beggi, F. Buscemi, and P. Bordone, "Quantum correlations of identical particles subject to classical environmental noise," *Quantum Information Processing*, vol. XX, no. X, pp. XXXX–XXXX, 2016. [Online]. Available: http://dx.doi.org/10.1007/XXXXXX
39. F. H. Essler, H. Frahm, F. Göhmann, A. Klümper, and V. E. Korepin, *The one-dimensional Hubbard model*. Cambridge University Press, 2005.
40. A. Montorsi, *The Hubbard Model: A Reprint Volume*. World Scientific, 1992.
41. E. H. Lieb and F. Wu, "The one-dimensional hubbard model: A reminiscence," *Physica A: Statistical Mechanics and its Applications*, vol. 321, no. 1, pp. 1–27, 2003.
42. L. Amico, R. Fazio, A. Osterloh, and V. Vedral, "Entanglement in many-body systems," *Rev. Mod. Phys.*, vol. 80, pp. 517–576, May 2008. [Online]. Available: http://link.aps.org/doi/10.1103/RevModPhys.80.517
43. P. M. Preiss, R. Ma, M. E. Tai, A. Lukin, M. Rispoli, P. Zupancic, Y. Lahini, R. Islam, and M. Greiner, "Strongly correlated quantum walks in optical lattices," *Science*, vol. 347, no. 6227, pp. 1229–1233, 2015. [Online]. Available: http://www.sciencemag.org/content/347/6227/1229.abstract
44. L.-M. Duan, E. Demler, and M. D. Lukin, "Controlling spin exchange interactions of ultracold atoms in optical lattices," *Phys. Rev. Lett.*, vol. 91, p. 090402, Aug 2003. [Online]. Available: http://link.aps.org/doi/10.1103/PhysRevLett.91.090402
45. T. Fukuhara, P. Schauß, M. Endres, S. Hild, M. Cheneau, I. Bloch, and C. Gross, "Microscopic observation of magnon bound states and their dynamics," *Nature*, vol. 502, no. 7469, pp. 76–79, 2013.
46. D. Jaksch and P. Zoller, "The cold atom hubbard toolbox," *Annals of Physics*, vol. 315, no. 1, pp. 52 – 79, 2005, special Issue. [Online]. Available: http://www.sciencedirect.com/science/article/pii/S0003491604001782

47. T. Fukuhara, A. Kantian, M. Endres, M. Cheneau, P. Schauß, S. Hild, D. Bellem, U. Schollwöck, T. Giamarchi, C. Gross *et al.*, "Quantum dynamics of a mobile spin impurity," *Nature Physics*, vol. 9, no. 4, pp. 235–241, 2013.
48. H. J. Schulz, "Correlation exponents and the metal-insulator transition in the one-dimensional hubbard model," *Phys. Rev. Lett.*, vol. 64, pp. 2831–2834, Jun 1990. [Online]. Available: http://link.aps.org/doi/10.1103/PhysRevLett.64.2831
49. Y. Lahini, M. Verbin, S. D. Huber, Y. Bromberg, R. Pugatch, and Y. Silberberg, "Quantum walk of two interacting bosons," *Phys. Rev. A*, vol. 86, p. 011603, Jul 2012. [Online]. Available: http://link.aps.org/doi/10.1103/PhysRevA.86.011603
50. Y. Bromberg, Y. Lahini, E. Small, and Y. Silberberg, "Hanbury brown and twiss interferometry with interacting photons," *Nature Photonics*, vol. 4, no. 10, pp. 721–726, 2010.
51. F. Lederer, G. I. Stegeman, D. N. Christodoulides, G. Assanto, M. Segev, and Y. Silberberg, "Discrete solitons in optics," *Physics Reports*, vol. 463, no. 1–3, pp. 1 – 126, 2008. [Online]. Available: http://www.sciencedirect.com/science/article/pii/S0370157308001257
52. C. Lee, A. Rai, C. Noh, and D. G. Angelakis, "Probing the effect of interaction in anderson localization using linear photonic lattices," *Phys. Rev. A*, vol. 89, p. 023823, Feb 2014. [Online]. Available: http://link.aps.org/doi/10.1103/PhysRevA.89.023823
53. S. Longhi, "Optical realization of the two-site bose-hubbard model in waveguide lattices," *arXiv preprint arXiv:1101.4762*, 2011.
54. T. Matsubara and H. Matsuda, "A lattice model of liquid helium, i," *Progress of Theoretical Physics*, vol. 16, no. 6, pp. 569–582, 1956.
55. X. Qin, Y. Ke, X. Guan, Z. Li, N. Andrei, and C. Lee, "Statistics-dependent quantum co-walking of two particles in one-dimensional lattices with nearest-neighbor interactions," *Phys. Rev. A*, vol. 90, p. 062301, Dec 2014. [Online]. Available: http://link.aps.org/doi/10.1103/PhysRevA.90.062301
56. ——, "Quantum walks of two interacting particles in one dimension," *arXiv preprint arXiv:1402.3349*, 2014.
57. L. Wang, L. Wang, and Y. Zhang, "Quantum walks of two interacting anyons in one-dimensional optical lattices," *Physical Review A*, vol. 90, no. 6, p. 063618, 2014.
58. L. Wang, N. Liu, S. Chen, and Y. Zhang, "Quantum walks accompanied by spin flipping in one-dimensional optical lattices," *Phys. Rev. A*, vol. 92, p. 053606, Nov 2015. [Online]. Available: http://link.aps.org/doi/10.1103/PhysRevA.92.053606
59. J. Hecker Denschlag and A. J. Daley, "Exotic atom pairs: Repulsively bound states in an optical lattice," in *Proceedings of the International School of Physics "Enrico Fermi"*, vol. 164. IOS Press Ebooks, 2007.
60. K. Winkler, G. Thalhammer, F. Lang, R. Grimm, J. H. Denschlag, A. Daley, A. Kantian, H. Büchler, and P. Zoller, "Repulsively bound atom pairs in an optical lattice," *Nature*, vol. 441, no. 7095, pp. 853–856, 2006.
61. L. Wang, Y. Hao, and S. Chen, "Preparation of stable excited states in an optical lattice via sudden quantum quench," *Phys. Rev. A*, vol. 81, p. 063637, Jun 2010. [Online]. Available: http://link.aps.org/doi/10.1103/PhysRevA.81.063637
62. S. Fölling, S. Trotzky, P. Cheinet, M. Feld, R. Saers, A. Widera, T. Müller, and I. Bloch, "Direct observation of second-order atom tunnelling," *Nature*, vol. 448, no. 7157, pp. 1029–1032, 2007.
63. R. Piil and K. Mølmer, "Tunneling couplings in discrete lattices, single-particle band structure, and eigenstates of interacting atom pairs," *Phys. Rev. A*, vol. 76, p. 023607, Aug 2007. [Online]. Available: http://link.aps.org/doi/10.1103/PhysRevA.76.023607
64. L. Wang, Y. Hao, and S. Chen, "Quantum dynamics of repulsively bound atom pairs in the bose-hubbard model," *The European Physical Journal D*, vol. 48, no. 2, pp. 229–234, 2008.
65. M. Valiente and D. Petrosyan, "Two-particle states in the hubbard model," *Journal of Physics B: Atomic, Molecular and Optical Physics*, vol. 41, no. 16, p. 161002, 2008.
66. A. Scott, J. Eilbeck, and H. Gilhøj, "Quantum lattice solitons," *Physica D: Nonlinear Phenomena*, vol. 78, no. 3, pp. 194–213, 1994.
67. D. Girolami and G. Adesso, "Interplay between computable measures of entanglement and other quantum correlations," *Phys. Rev. A*, vol. 84, p. 052110, Nov 2011. [Online]. Available: http://link.aps.org/doi/10.1103/PhysRevA.84.052110
68. S. Lee, D. P. Chi, S. D. Oh, and J. Kim, "Convex-roof extended negativity as an entanglement measure for bipartite quantum systems," *Phys. Rev. A*, vol. 68, p. 062304, Dec 2003. [Online]. Available: http://link.aps.org/doi/10.1103/PhysRevA.68.062304
69. U. Schneider, L. Hackermüller, J. P. Ronzheimer, S. Will, S. Braun, T. Best, I. Bloch, E. Demler, S. Mandt, D. Rasch *et al.*, "Fermionic transport and out-of-equilibrium dynamics in a homogeneous hubbard model with ultracold atoms," *Nature Physics*, vol. 8, no. 3, pp. 213–218, 2012.
70. ——, "Breakdown of diffusion: From collisional hydrodynamics to a continuous quantum walk in a homogeneous hubbard model," *arXiv preprint arxiv:1005.3545*, 2010.
71. T. Chattaraj and R. V. Krems, "Effects of long-range hopping and interactions on quantum walk in ordered and disordered lattices," *arXiv preprint arXiv:1605.04349*, 2016.